SEISMIC DEPTH PROCESSING USING THE CRS TECHNIQUE - A 3D LAND DATA EXAMPLE FROM MEXICO

L. Freitas, R. Ballesteros, A. Caballero, G. Gierse, J. Pruessmann, A. Vazquez, and G. Clemente

email: *lucas.batista.freitas@gmail.com*

keywords: *CRS method, depth processing, model building, practical applications*

ABSTRACT

A case study for a 3D land data from Mexico illustrates the contributions that CRS attributes may bring to important steps of depth processing.
The first contribution of CRS attributes lies on initial depth model building. The CRS tomographyic inversion can be easily appended to Dix inversion resulting in a initial model with better correspondence with the subsurface structures. A poststack depth migration of CRS stack volume also yields a higher quality initial depth image, fundamental for starting salt body delimitation. The use of CRS attributes for generating CRS gathers provide higher quality data for PSDM

INTRODUCTION

Seismic depth processing is the decisive step to reconstruct the structural geometry in the subsurface. Depending on the desired accuracy, the depth model building and the depth imaging can be very time-consuming and costly steps. In order to increase the depth resolution and signal quality especially in data of varying fold or quality, the CRS technique can be integrated at some crucial stages of the general depth imaging procedure.

In this case study, a depth processing is based on the initial CRS time processing of 3D seismic land data from Mexico. At the surface, the acquisition of this data had to deal with several inhabited areas that caused strong variations of fold and of data quality. In the subsurface, the Tertiary and Mesozoic sediments are disturbed by strong salt tectonics in part of the survey. The low fold areas and the complicated subsurface represented the main challenges for depth processing.

The CRS time processing provides volumes of both the CRS image and the CRS stacking parameter or attributes. Among the several uses of such attributes, are multiple suppression described by F. Gamboa and Tygel (2003) and Dümmong et al. (2008), poststack redatuming showed by Z. Heilmann and Koglin (2006)), and residual statics calculation presented by Koglin (2001).

In this paper, we show how three distinguished applications of CRS attributes can bring important contributions for the depth processing, reducing the number of iterative velocity model building cycles. They are CRS tomography, proposed by Duveneck (2004), for initial depth model building; CRS stack, as described by Müller (2003), for initial depth imaging through PostSDM; and CRS gathers, proposed by Baykulov and Gajewski (2008), for enhancing the pre-stack data quality for PSDM iterative and model update.

GEOLOGICAL SETTING AND EXPLORATION OBJECTIVES

The onshore study area is located in the Salina del Istmo Basin in Mexico, south of the Gulf of Mexico and in the northern part of the Istmo of Tehuantepec (Figure 1). This basin covers parts of the states of Veracruz and of Chiapas, in southern Mexico. Several producing oil fields are located in this area, such

Figure 1: Location of the survey

as Sanchez Magallanes, Blasillo, San Ramon, and Cinco Presidentes. Lithologically, these oil fields are associated with Miocene sands. Their structures are dominated by strong salt tectonics.

For this case study, a 3D reflection seismic data set is selected from an onshore survey that was acquired in the 1990s in the Salina del Istmo Basin. With maximum offsets of about 3800 meters in inline direction and 3200 meters in crossline direction, the seismic acquisition originally targeted shallow structures at a depth no higher than 3 kilometers.

The CRS-enhanced depth imaging now aimed not only at deeper targets and subsalt structures down to the Mesozoic level, but also at a better fault definition in the shallow Tertiary sediments. The limited offset, a low signal-to-noise ratio, and low fold in inhabited areas posed the major difficulties to be overcome.

THE CRS METHOD

In the time processing, the CRS or Common-Reflection-Surface method was applied in order to compensate for the imaging problems in the low-fold areas as well as increase dataset's signal-to-noise ratio. The processing steps that preceded the CRS are the ones from a standard time workflow until the final application of residual statics and, therefore, are not in the scope of this work, for more details in such topic refer to Yilmaz (2000).

The CRS stack, as described by Tygel et al. (1997) and Müller (1999), is a technique which aims to obtain optimum simulated zero-offset volumes by stacking the multicoverage dataset along multi-parameter surfaces determined in a data-driven way. The stacking operator is of second order in the half-offset and midpoint coordinates. Thus, for each zero-offset sample to be simulated, stacking is performed not only along a trajectory restricted to the one CMP gather but along an entire surface in time-midpoint-offset space, locally approximating the corresponding traveltime surface in the prestack data over several CMPs. The much higher stacking fold results in a significantly improved S/N ratio.

CRS stacking operators depend on a number of parameters called CRS attributes, kinematic wavefield attributes or wavefront attributes which determine their shapes. In the 3D case, the three CRS attributes are denoted by two 2×2 symmetric matrices $\mathbf{M}_\xi$ and $\mathbf{M}_h$, and 1×2 vector $\mathbf{p}$ which are the traveltime derivatives. The CRS operator, computed in midpoint and half-offset coordinates $(\boldsymbol{\xi}, \mathbf{h})$ in the vicinity of a zero-offset trace $\boldsymbol{\xi} = \boldsymbol{\xi}_0$, $\mathbf{h} = \mathbf{0}$ is given by

$$t^2(\boldsymbol{\xi}, \mathbf{h}) = [t_0 + 2\mathbf{p}^T(\boldsymbol{\xi} - \boldsymbol{\xi}_0)]^2 + 2t_0[(\boldsymbol{\xi} - \boldsymbol{\xi}_0)^T \mathbf{M}_\xi (\boldsymbol{\xi} - \boldsymbol{\xi}_0) + \mathbf{h}^T \mathbf{M}_h \mathbf{h}] \,. \tag{1}$$

where t_0 is the traveltime of the zero-offset ray that emerges at $\boldsymbol{\xi}_0$.

Therefore, associated to the simulated zero-offset volume there are a number of attribute volumes (three volumes in 2D and eight in 3D). These volumes consist in the optimum attribute values determined by means of coherence analysis.

As described by Müller (2003), these traveltime derivatives contain information about the normal ray and the so called eigenwaves defined by Hubral (1983). These are two hypothetical waves that start at the normal-incident point (NIP) and propagate upwards with half the medium velocity: the NIP wave

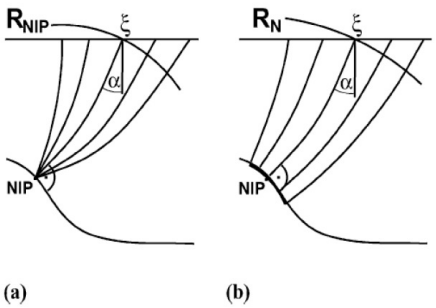

Figure 2: 2D diagram of (a) the NIP wave,and(b)the N-wave

propagates from a point source; while the N wave propagates from an exploding reflection element (see Figure 2 for a 2D diagram).

The first order derivative estimated for a zero-offset sample $(\boldsymbol{\xi}_0, t_0)$ relates to the emergence angles of the normal ray which emerges at $\boldsymbol{\xi}_0$, and has two-way traveltime t_0. The second order derivatives, on the other hand, give information about the curvature of the associated eigenwaves observed at $\boldsymbol{\xi}_0$. More specifically,

$$\mathbf{p} = \frac{1}{2}\frac{\partial t}{\partial \xi} = \frac{1}{v_0}[\sin(\alpha)\cos(\phi), \sin(\alpha)\sin(\phi)]^T$$

$$\mathbf{M}_h = \frac{1}{2}\frac{\partial^2 t}{\partial h^2} = \frac{1}{v_0}\mathbf{H}\mathbf{K}_{\text{NIP}}\mathbf{H}^T$$

$$\mathbf{M}_\xi = \frac{1}{2}\frac{\partial^2 t}{\partial \xi^2} = \frac{1}{v_0}\mathbf{H}\mathbf{K}_{\text{N}}\mathbf{H}^T$$

where is the near-surface velocity, and $\mathbf{H}$ is the transformation matrix from measured surface coordinates to local ray-centered Cartesian coordinates determined by two subsequent rotations in azimuth (ϕ) and dip (α) direction.

In this case study, the attribute volumes obtained by the CRS time processing have contributions in three major steps of depth processing: (a) initial depth model building by CRS tomography; (b) initial depth model update; and (c) PSDM by increasing the signal-to-noise ratio of the pre-stack data by CRS gathers.

INITIAL DEPTH MODEL BUILDING

Velocity model building using iterative prestack depth migration requires many runs of computationally-intensive prestack depth migration. Thus, a good initial depth model is crucial for an efficient depth processing procedure. In this case study, three different model building approaches based in time processing were performed:

- Dix inversion of RMS velocities
- Tomographic inversion
  - layer-based
  - grid-based

Dix inversion

In standard seismic processing, the RMS velocities are approximated from stacking velocities for the purpose of time migration. The Dix formula, presented by Dix (1955), transforms RMS velocities to interval velocities. The principal inherent assumption is that the subsurface is composed of flat layers with homogeneous velocities that generate hyperbolic moveout.

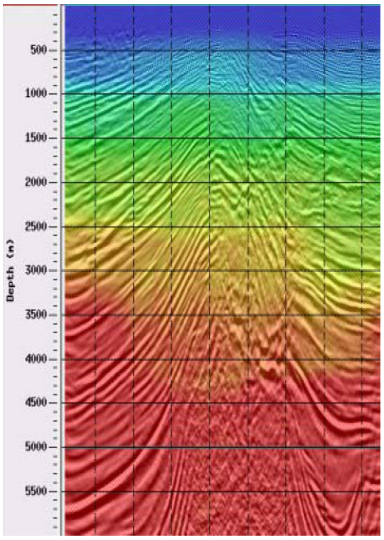

Figure 3: Initial model by Dix inversion

The advantage of the Dix transform method is that it is simple, so it is usually appended to any normal time processing. This is also its disadvantage. First, it does not account for the non-hyperbolic moveout introduced by lateral velocity variations within the offset range. For this reason, RMS velocities are said to be the near-offset stacking velocities. Second, because RMS velocity is a time-average velocity, it does not account for raypath bending. Third, it does not account for the effect of structural dip (DMO transformation of time gathers will diminish, but not eliminate this error).

In this case study, the deviation of the Dix model from the depth structure in an associated postSDM volume was obvious even in regions of good data quality (Figure 3)

Tomographic inversion

Because of its technical qualities, tomographic inversion has emerged as the most favored method for model refinement. It seeks a global solution for minimizing residual moveout in a least-squares sense. Most of the other methods work in a layer-stripping manner i.e., it is assumed that the velocity in the overburden above the point in concern has been perfectly resolved, and only the target layer is refined. In contrast, global tomography does not suffer from this limitation. Refinements can be made anywhere within the model. Moreover, the depth model refinement corresponding to the velocity model refinement can be simultaneously implemented in the framework of tomographic inversion

Layer-based tomography In the layer-based approach, as described by Stork (1992), the velocities are estimated utilizing a structural framework of geologic horizons, which enables the portrayal of velocity changes caused by depth, age, lithology, and pressure. The advantage of this approach is that it enables the image to more explicitly account for the raypath bending effects of complex structures. The disadvantage is that a priori knowledge of the structure is needed. In practice, traveltime picking can be a difficult and fastidious operation, since picked events have to be identified all over the traces in the dataset, even where the signal-to-noise ratio is very low. The major problem is the labor-intensive nature of reflector picking, especially in 3-D data.

For the layer-based approach, several key horizons were provided from interpretation in time (Figure 4). Interpretation, however, severely suffered from areas with acquisition gaps and low-quality data, and left large parts of the horizons undefined. These missing parts could not easily be interpolated due to the strong structural variations. As a result, the layer-based model building by map migration did not lead to reasonable results for this data configuration.

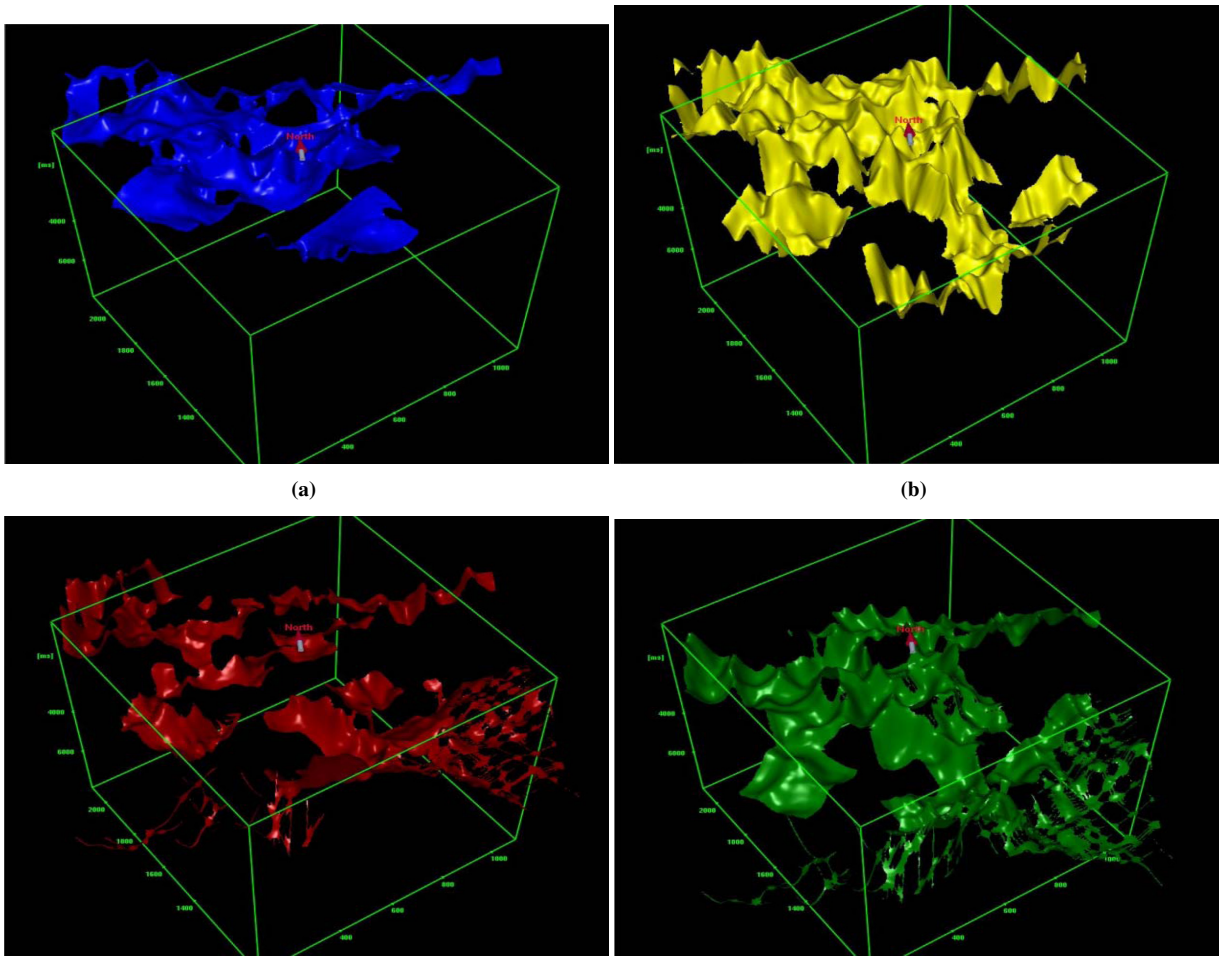

(a) **(b)**

(c) **(d)**

Figure 4: Interpreted horizons (from top to bottom): Pliocene, top-salt, Miocene and cretaceous

Grid-based tomography In the grid-based approach, velocities are estimated without regard to the structure framework. Therefore, a priori knowledge of the structure is not required. This method is most suitable when the depth of burial and the age of the sedimentary formations are important factors controlling the velocity other than the lithology, and is widely used in the Gulf of Mexico. That is because the use of a grid-based model allows the definition of lateral and vertical velocity gradients. Another situation where the grid-based approach may prove useful is where structure is so complex that the seismic data yields few clues for deriving an a priori structural framework. In these cases, the flexibility of picking locally coherent reflection events turns to be its major advantage over the layer-based approach.

Among the several methods of grid-based tomography, CRS tomography has a distinct role. As a variation of slope tomography, it has a distinguished advantage over the other approaches: its traveltime picking. Dümmong et al. (2008) emphasize that picking in CRS tomography is drastically simplified by being performed in the poststack domain with much higher signal-to-noise ratio..

Proposed by Duveneck (2004), the CRS tomography uses the concept of focusing a NIP wavefront back to its hypothetical source, as proposed by Hubral and Krey (1980), for this reason is also called NIP wave tomography.

The emerging NIP wavefront is characterized by four parameters: the traveltime t_0, emergency location $\boldsymbol{\xi}$, emergence azimuth ϕ and dip α of the normal ray, and the 2x2 simmetric curvature matrix of the NIP wavefront at $\boldsymbol{\xi}$, $\mathbf{K}_{\text{NIP}}$.

The charm of this tomographic approach lies on the simplified manner of determining the input data. The first two features are determined by means of the coherence-based automatic picking proposed by Koglin (2001), and subsequent outlier elimination. The other two parameters are obtained in a straightforward manner by accessing the attribute volumes.

Despite having limitations when compared to other grid-based tomographic inversion methods, NIP wave tomography provides a good option for tomography since these limitations are compensated by the little human intervention, as mentioned by Dümmong et al. (2008) and Duveneck (2004).

As mentioned above, Dix inversion consists in a direct application of the stacking velocity, the key parameter for CMP stacking. In an analogous manner, NIP wave tomography can be seen as a direct application of the CRS attributes. As CRS time processing is considered as a stacking methodology beyond the CMP by Hertweck et al. (2007), NIP wave tomography can be seen as the CRS corresponding of initial model building, beyond Dix inversion.

In this case study, the automatic event picking was performed on selected traces on a rectangular grid. These event picks and the associated CRS attributes then were used in the iterative inversion by NIP wave tomography. Very strong smoothing of the Dix velocities was used as a starting model which was then refined by ten iterations of the inversion step.

The CRS tomographic model is compared to its initial model obtained by Dix, at an inline position, along with the respective poststack depth migration of the CRS stack (Figure 5). Note the better correspondence to the subsurface structures after the tomographic refinement. Just like the other flat-layer methods, Dix inversion is a local method, it solves 1D velocity profiles, which are then combined with smoothing to produce a 3D model. In contrast, CRS tomography, as a tomographic method, is a global method, so the smoothness constraints are built directly into the 3D solution of the residual equations.

Pruessmann et al. (2008) shows additional approached for further confirmation of the CRS tomography model by well calibration, and by analysis of the common-image gathers in prestack depth migration .

MODEL UPDATE

Following the typical workflow for sub-salt imaging of Mosher et al. (2007); once the sediment velocity field had been determined, an initial depth image was used to determine the position of the top-salt, below which salt velocity is inserted and extended vertically - a procedure referred to as salt-flood.

Top-salt definition

In this case study, the initial depth image was obtained by postSDM. As already mentioned, and illustrated in Figure 6, stacking along the CRS operator provides stack volumes with much higher signal-to-noise

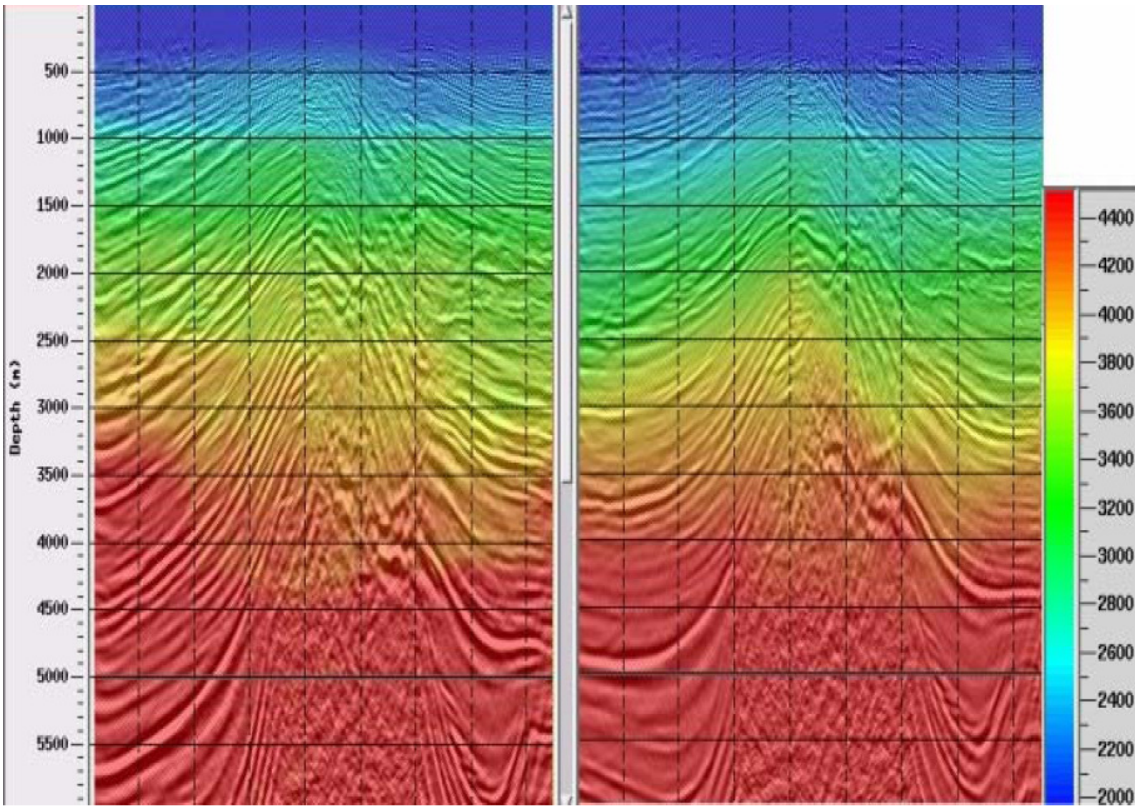

Figure 5: Comparison of the initial model determined by Dix inversion (left) and by CRS tomography (right).

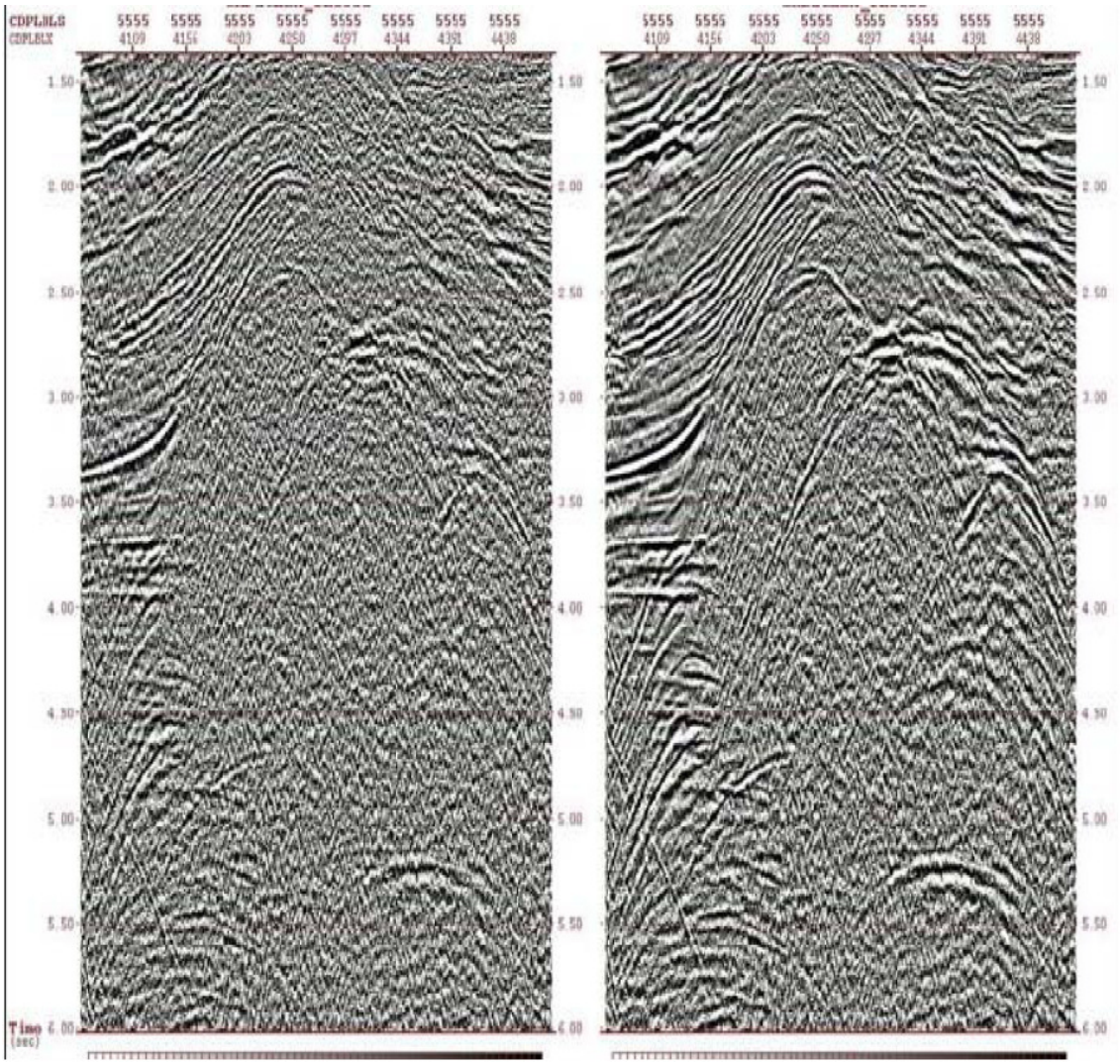

Figure 6: Detail of stacking volumes over a single CMP (left) and the CRS operator (right)

ratio. Subsequent poststack migration of these volumes, consequently lead to depth images of very good quality. In some situations, such results are even comparable to usual PSDM images (Figure 7).

Salt-body delimitation and PSDM

After salt-flooding, the rest of the salt-body is delimited by successive PSDM in an iterative manner as described by Albertin et al. (2001).

CRS Gather As mentioned above, the CRS methodology is based on a second order approximation of the reflection event on both half-offset and midpoint coordinates. A schematic description of both iso-offset curves of traveltime, in blue, and the CRS approximation, in green is presented in Figure 8

The CRS gather proposed by Baykulov and Gajewski (2008) is generated by partial stacking along the midpoint direction, i.e., along the red lines in Figure 8 . In practice, it is determined in two steps: First, a moveout corrected gather is extracted from the dataset by direct application of the CRS attributes and stacking only in the midpoint direction. Then conventional moveout recovery and regularization is applied. As expected, the generated gathers present an excelent signal-to-noise ratio when compared to the input

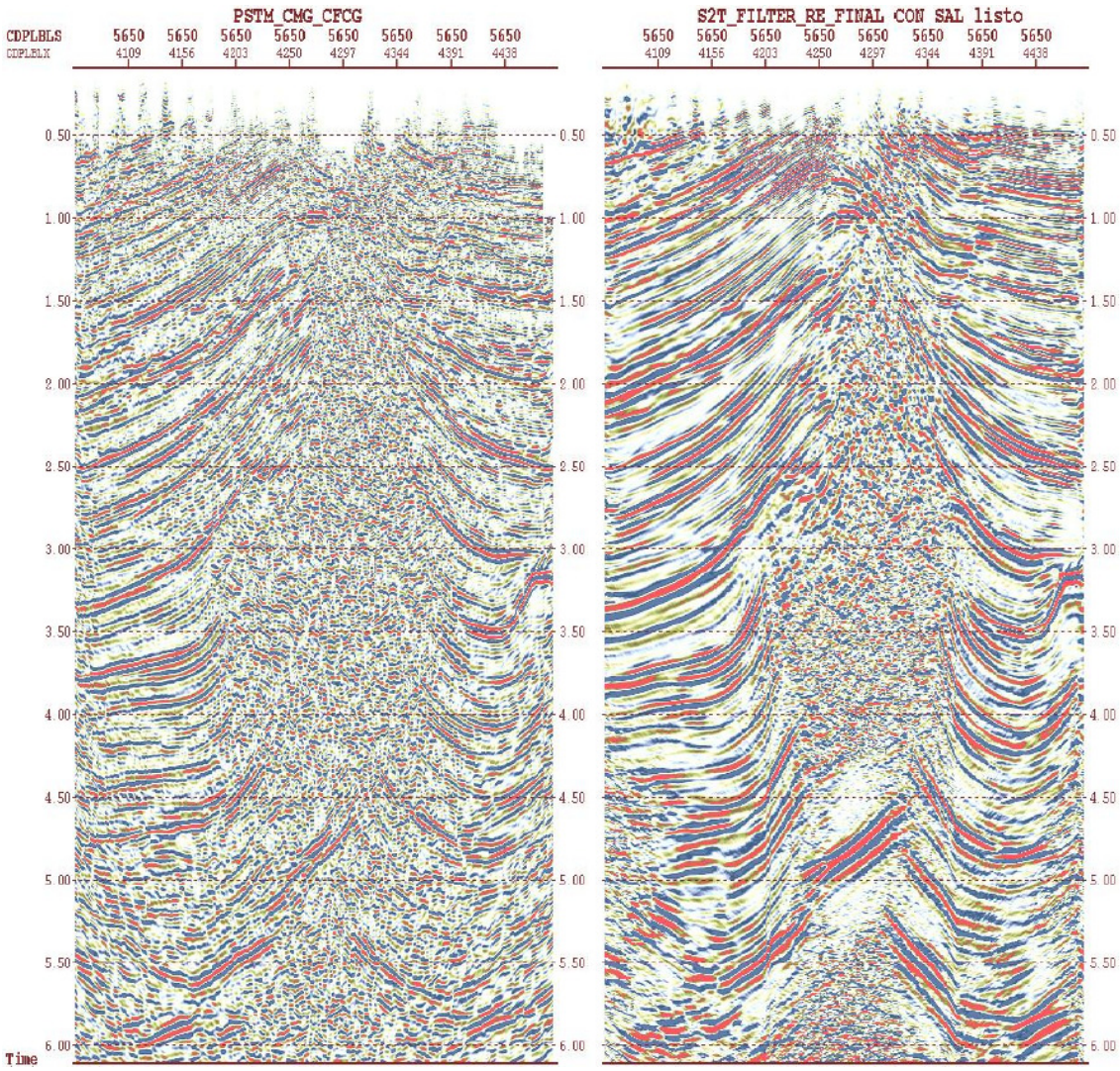

Figure 7: Comparison of PSDM from another project (left) and PostSDM of CRS stack (right). Note that both processing sequences started from the same pre-processed CMP gathers.

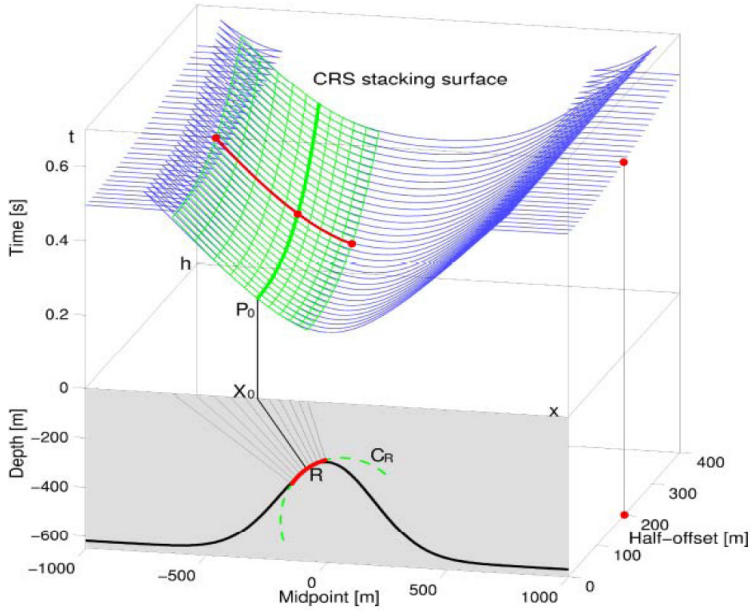

Figure 8: Illustration of the CRS operator (green) and the partial stacking for a given offset (red).

CMP gathers (Figures 9 and 10).

The last major contribution of CRS technique in the depth imaging workflow is the CRS gather. The excellent enhance it provides to the input prestack gather leads to both an easier definition of the final model and a better quality depth image result.

Using the CRS gathers as input for the PSDM on the iterative model update, we reached the final model illustrated in Figure 11. It basically consists of the incorporation of the salt-body into the smooth model derived from CRS tomography.

The depth imaging reaches its end by performing PSDM over the CRS gathers using the final model illustrated in Figure 11. As illustrated in Figure 12, such depth image presents much more definition of both salt-body and sediment reflectors when compared to the image from another project.

CONCLUSIONS

This case study shows how the CRS technique may be incorporated into well established depth imaging workflow by means of CRS attributes applications. CRS tomography, as a robust and automatic inversion procedure, may be directly appended to Dix-based inversion resulting in much better initial velocity models, reducing the number of model update cycles considerably. CRS stack volumes, when migrated to depth, provide very good initial depth images, suitable for top-salt delimitation. CRS gathers, as an enhanced prestack data, not only facilitates the iterative model update process but also leads to final depth images of much higher quality.

ACKNOWLEDGMENTS

We than PEMEX for the permission to present their data.

REFERENCES

Albertin, U., Woodward, M., Kapoor, J., Chang, W., Charles, S., Nichols, D., Kitchenside, P., and Mao, W. (2001). Depth imaging examples and methodology in the gulf of mexico. *The Leading Edge*, 20(5):498–513.

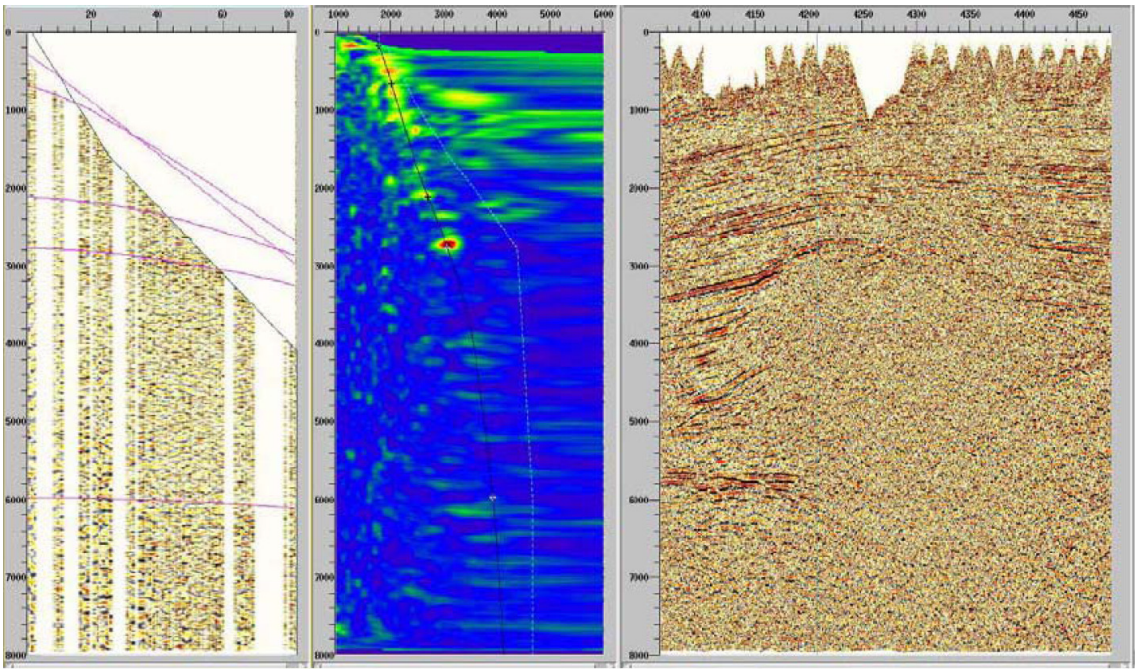

Figure 9: A CMP gather, its semblance panel an the stack section for one inline.

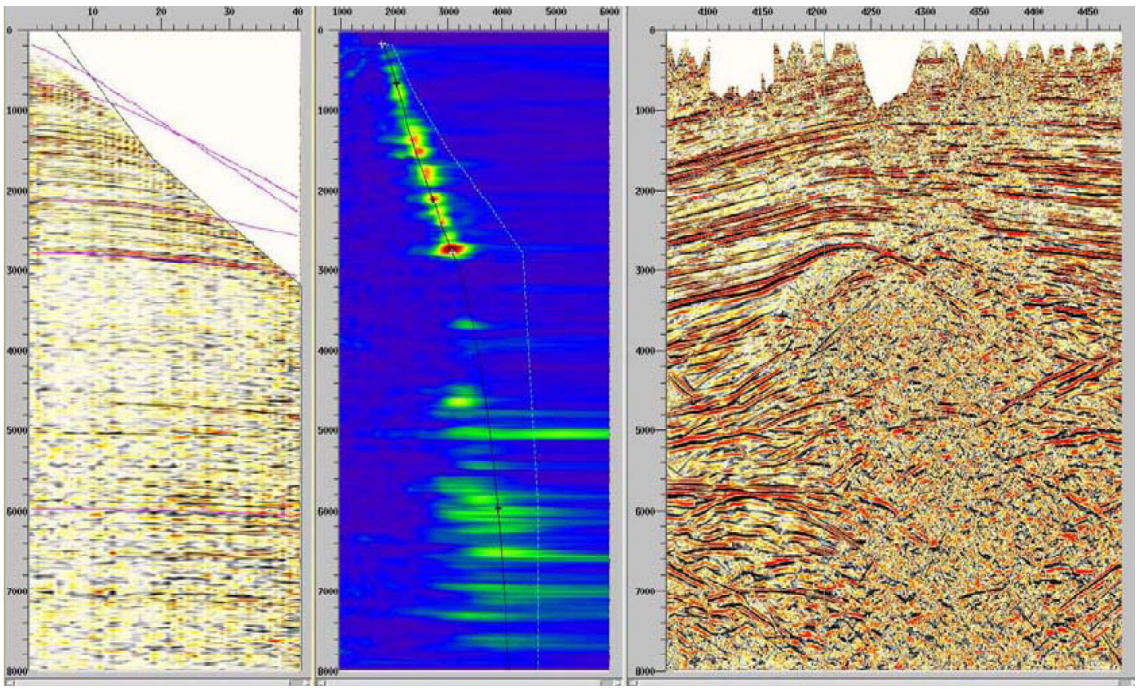

Figure 10: The CRS gather, its semblance panel and the stack section for the same locations of Figure 9.

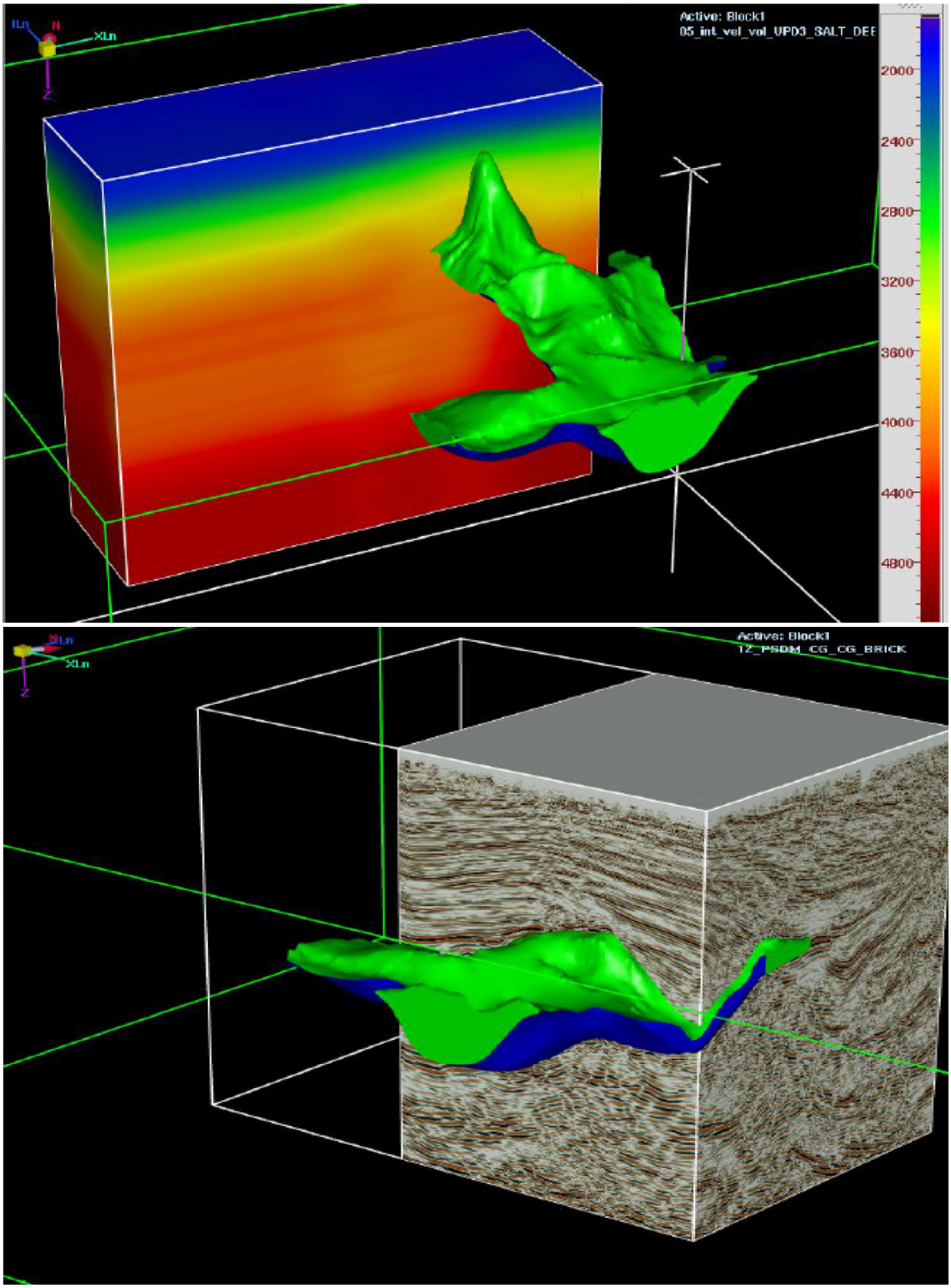

Figure 11: Final depth model. Interval velocities with salt-body interpretation (top) and depth image with salt-body interpretation (bottom).

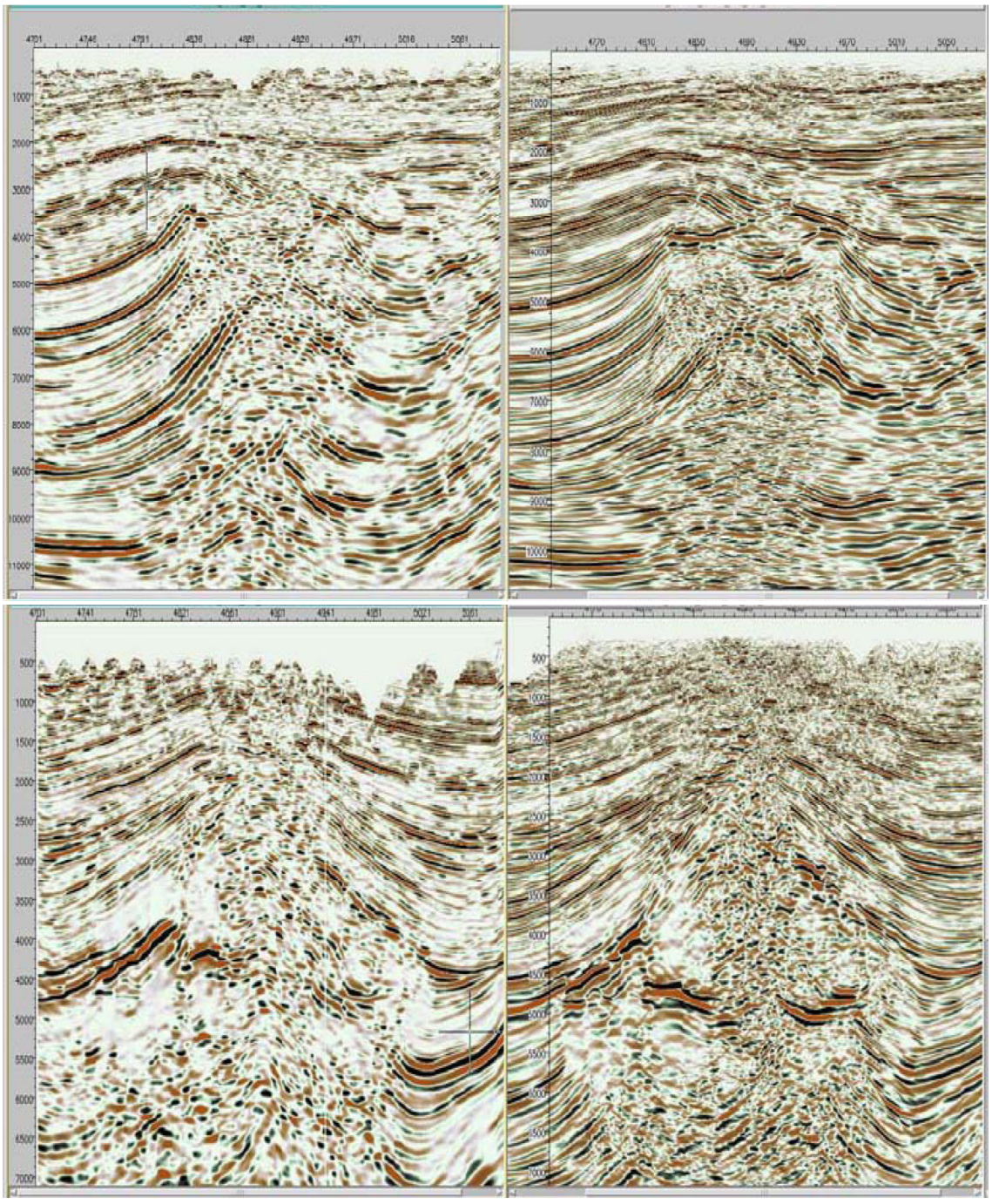

Figure 12: PSDM comparison: Note the excellent definition of the pinch-out, faults, and sedimentary events from the Tertiary on the result from the proposed workflow (upper right) when compared to the result from a previous project (upper left). On another inline, the proposed methodology also presents a much more definition of salt-bottom (bottom right) when compared to the previous project (bottom left).

Baykulov, M. and Gajewski, D. (2008). Prestack seismic data enhancement with crs parameters. In *70th EAGE Conference and Exhibition Ext. Abstr*, Rome.

Dix, C. H. (1955). Seismic velocities from surface measurements. *Geophysics*, 20(1):68–86.

Dümmong, S., Meier, K., Gajewski, D., and Hübscher, C. (2008). Comparison of prestack stereotomography and nip wave tomography for velocity model building: Instances from the messinian evaporites. *Geophysics*, 73(5):VE291–VE302.

Duveneck, E. (2004). Velocity model estimation with data-derived wavefront attributes. *Geophysics*, 69(1):265–274.

F. Gamboa, E. F. and Tygel, M. (2003). Multiple attenuation using common-reflection-surface attributes. *Rev. Bras. Geof. [online]*, 21(1):43–51.

Hertweck, T., Schleicher, J., and Mann, J. (2007). Data stacking beyond cmp. *The Leading Edge*, 26(7):818–827.

Hubral, P. (1983). Computing true amplitude reflections in a laterally inhomogeneous earth. *Geophysics*, 48(8):1051–1062.

Hubral, P. and Krey, T. (1980). *Interval velocities from seismic reflection time measurements*. Society of Exploration Geophysics.

Koglin, I. (2001). Picking and smoothing of seismic events and crs attributes and application for inversion. Master's thesis, Karlsruhe University.

Mosher, C., Keskula, E., Malloy, J., Keys, R., Zhang, H., and Jin, S. (2007). Iterative imaging for subsalt interpretation and model building. *The Leading Edge*, 26(11):1424–1428.

Müller, A. (2003). *The 3D Common Reflection Surface: Theory and Application*. PhD thesis, Karlsruhe University.

Müller, T. (1999). *The common reflection surface stack method*. PhD thesis, Karlsruhe University.

Pruessmann, J., Frehers, S., Ballesteros, R., Caballero, A., and Clemente, G. (2008). Crs-based depth model building and imaging of 3d seismic data from the gulf of mexico coast. *Geophysics*, 73(5):VE303–VE311.

Stork, C. (1992). Reflection tomography in the postmigrated domain. *Geophysics*, 57(5):680–692.

Tygel, M., Müiller, T., Hubral, P., and Schleicher, J. (1997). Eigenwave based multiparameter traveltime expansions. *SEG Technical Program Expanded Abstracts*, 16(1):1770–1773.

Yilmaz, O. (2000). *Seismic data analysis*. Soc. of Expl. Geophys.

Z. Heilmann, J. M. and Koglin, I. (2006). Crs-stack-based seismic imaging considering top-surface topography. *Geophys. Prosp.*, 54(6):681–695.